NASA/TM—2019-219999

Fatigue Behavior of Coated Titanium Alloys

Dongming Zhu and Bradley A. Lerch
Glenn Research Center, Cleveland, Ohio

Sreeramesh Kalluri
Ohio Aerospace Institute, Brook Park, Ohio

June 2019

NASA STI Program . . . in Profile

Since its founding, NASA has been dedicated to the advancement of aeronautics and space science. The NASA Scientific and Technical Information (STI) Program plays a key part in helping NASA maintain this important role.

The NASA STI Program operates under the auspices of the Agency Chief Information Officer. It collects, organizes, provides for archiving, and disseminates NASA's STI. The NASA STI Program provides access to the NASA Technical Report Server—Registered (NTRS Reg) and NASA Technical Report Server—Public (NTRS) thus providing one of the largest collections of aeronautical and space science STI in the world. Results are published in both non-NASA channels and by NASA in the NASA STI Report Series, which includes the following report types:

- TECHNICAL PUBLICATION. Reports of completed research or a major significant phase of research that present the results of NASA programs and include extensive data or theoretical analysis. Includes compilations of significant scientific and technical data and information deemed to be of continuing reference value. NASA counter-part of peer-reviewed formal professional papers, but has less stringent limitations on manuscript length and extent of graphic presentations.

- TECHNICAL MEMORANDUM. Scientific and technical findings that are preliminary or of specialized interest, e.g., "quick-release" reports, working papers, and bibliographies that contain minimal annotation. Does not contain extensive analysis.

- CONTRACTOR REPORT. Scientific and technical findings by NASA-sponsored contractors and grantees.

- CONFERENCE PUBLICATION. Collected papers from scientific and technical conferences, symposia, seminars, or other meetings sponsored or co-sponsored by NASA.

- SPECIAL PUBLICATION. Scientific, technical, or historical information from NASA programs, projects, and missions, often concerned with subjects having substantial public interest.

- TECHNICAL TRANSLATION. English-language translations of foreign scientific and technical material pertinent to NASA's mission.

For more information about the NASA STI program, see the following:

- Access the NASA STI program home page at http://www.sti.nasa.gov

- E-mail your question to help@sti.nasa.gov

- Fax your question to the NASA STI Information Desk at 757-864-6500

- Telephone the NASA STI Information Desk at 757-864-9658

- Write to:
  NASA STI Program
  Mail Stop 148
  NASA Langley Research Center
  Hampton, VA 23681-2199

NASA/TM—2019-219999

Fatigue Behavior of Coated Titanium Alloys

Dongming Zhu and Bradley A. Lerch
Glenn Research Center, Cleveland, Ohio

Sreeramesh Kalluri
Ohio Aerospace Institute, Brook Park, Ohio

National Aeronautics and
Space Administration

Glenn Research Center
Cleveland, Ohio 44135

June 2019

Acknowledgments

This work was supported by the NASA Aeronautics Program Supersonics Project and the NASA Transformational Tools and Technologies Project. The authors are grateful to Dr. Ronghua Wei of Southwest Research Institute in helping the coating processing with the plasma enhanced magnetron sputtering (PEMS) physical vapor deposition, and to Laura Evans of NASA Glenn Research Center for her assistance with the scanning electron microscopy (SEM) and energy dispersive spectroscopy (EDS) analysis.

In particular, we would like to express appreciation for the contributions of our late friend, colleague, and co-author, Dr. Dongming Zhu.

Level of Review: This material has been technically reviewed by technical management.

Available from

NASA STI Program
Mail Stop 148
NASA Langley Research Center
Hampton, VA 23681-2199

National Technical Information Service
5285 Port Royal Road
Springfield, VA 22161
703-605-6000

This report is available in electronic form at http://www.sti.nasa.gov/ and http://ntrs.nasa.gov/

Fatigue Behavior of Coated Titanium Alloys

Dongming Zhu and Bradley A. Lerch
National Aeronautics and Space Administration
Glenn Research Center
Cleveland, Ohio 44135

Sreeramesh Kalluri
Ohio Aerospace Institute
Brook Park, Ohio 44142

Summary

Advanced multicomponent TiAlCrTaSiN-based multilayered coatings were developed and processed onto Ti-6Al-4V (Ti-6-4) and GammaMet PX (GMPX, or TiAl) alloys by a plasma-enhanced magnetron sputtering physical vapor deposition technique. The coatings have recently been in development with the goal of improving the advanced titanium alloy, turbine engine component durability, and oxidation-erosion resistance. In this work, the performance of the multicomponent coating system (including the outer-layer nitride-based coating and inner TiAlCrSi oxidation barrier bond coat) was studied, and the coating's effects on the fatigue behavior of the titanium-based alloys were compared. Although the multicomponent coating was initially optimized to improve the coating's high-temperature oxidation and erosion resistance, the lower ductility nitride-based coating needs further work on microstructure or composition to improve its mechanical stress resistance and strain tolerance to be used in cyclically loaded turbine blade applications. This is particularly true for GMPX and other γ-TiAl alloys because these intermetallic titanium alloys have limited ductility and are very sensitive to defects such as coating cracks. However, it was found that the inner-layer TiAlCrSi coating had good adhesion and ductility, and may be a suitable choice for improving the oxidation resistance of titanium alloys.

Introduction

Advanced titanium alloys, such as Ti-6Al-4V (Ti-6-4) and GammaMet PX (GMPX, or TiAl), are of great interest for aircraft engine turbine components because of their high specific strength and good fatigue and creep resistance. The intermetallic-based GMPX and other gamma TiAl alloys have significantly improved high-temperature stiffness and tensile and creep strengths (Refs. 1 and 2). However, the main issue with these intermetallic alloys is their limited ductility and fracture toughness compared to standard titanium alloys, particularly at higher use temperatures. Moreover, although TiAl has good strength at high temperatures, its usage limits are restricted in oxidizing environments because of oxygen dissolution in the TiAl alloys (Refs. 1 and 2). The present study was undertaken to examine the performance of a multicomponent titanium aluminum nitride-based coating system and its influence on the fatigue behavior of titanium-based alloys. Two titanium alloys, Ti-6-4 and GMPX, were examined. These alloys were chosen because samples already existed from prior NASA programs since they are of interest for use in lightweight low-pressure turbine and compressor blade applications and because some fatigue data on these two uncoated alloys already exist. Additionally, these two alloys also represent two of the titanium alloy categories—alpha-beta alloy and intermetallic TiAl alloy systems—which behave in distinctly different manners because of their crystal structures.

Titanium-nitride-based coatings have been widely used for applications requiring high hardness and toughness (Refs. 3 and 4). Additional alloy additions and architectural designs can further improve their toughness and oxidation resistance (Ref. 3). These alloy modifications can easily be made because of recent processing developments in physical vapor deposition (PVD), which has shown its potential of incorporating multiple elements such as Cr and Si to improve overall toughness and thermal stability (Ref. 4). Previous work has been performed on these coating systems to enhance oxidation resistance and erosion (Ref. 5). Various substrates were involved in addition to titanium, including SiC/SiC ceramic matrix composites, which have potential to be combustor and turbine vane materials. A processing study had previously been performed on various coatings, and the best was selected through a design of experiments (DOE) investigation based on earlier erosion and oxidation screening tests. The titanium-based, multicomponent coating was a further advancement based on the down-selected system from the original study. This coating showed beneficial effects for a GMPX TiAl alloy by improving its ductility under tension and creep in oxidizing environments.

The understanding of how these coatings respond to high imposed loads and cyclic strains as would be experienced in turbine operating conditions is crucial. Whereas coatings often are designed for improved oxidation resistance, they often fall short when external loads are applied, leading to coating cracks and spallation. This is especially critical in intermetallic alloys since they have limited ductility and fracture toughness. Any defect, such as a coating crack, can easily propagate into the substrate and result in premature fracture. Hence, this study takes a first look at the durability of these coatings on both ductile and nonductile substrates to further enhance coating development.

Experimental Materials and Procedures

The multicomponent TiAlCrTaSiN system was formed by co-depositing the multiple target alloy elements Ti, Al, Cr, and Ta along with silane (Si) and N_2 gas by a plasma enhanced magnetron sputtering (PEMS) PVD technique, processed at Southwest Research Institute (SwRI, TX) under a NASA contract. A two-layer coating system was employed. The initial layer was a thin metallic-rich TiCrAlSi layer (less than 5 μm thick) on the alloy substrate, which acted as the bond coat and to ensure oxidation protection and restrict embrittlement of the titanium alloys. A subsequent TiCrAlTaSiN layer (less than 15 μm thick) was then deposited onto the bond coat, acting as a top coating to improve erosion and impact resistance. One TiAl sample was given a pretest oxidation treatment of 100 h at 800 °C in air.

Flat fatigue samples were used for fatigue endurance testing on both alloys. The Ti-6Al-4V alloy specimens were machined from supplied 3.2-mm- (1/8-in-) thick rolled sheets, whereas the GMPX TiAl specimens were fabricated from forged plate (Refs. 1 and 2). The samples were 152.4 mm (6 in.) in length and 12.7 mm (0.5 in.) wide in the grip areas. The test specimen thickness was 3.2 mm (0.125 in.) for the Ti-6-4 and 2.1 mm (0.081 in.) for the TiAl. All samples had a machined dog-bone gage section with nominal gage dimensions of 10 by 25.4 mm (0.39 by 1 in.). Unlike the rectangular shape of the Ti-6-4 specimens the TiAl samples had machined, beveled edges that were intended to simulate the leading-edge profile of low-pressure turbine blades (Figure 1) (Ref. 1). The Ti-6-4 samples were tested in the annealed condition. Fifteen Ti-6-4 alloy samples were fatigue tested, seven uncoated and eight coated. Ten TiAl alloy samples were tested, three uncoated and seven coated. Fatigue tests were conducted at 427 °C (Ti-6-4) and 650 °C (TiAl) in air at a frequency of 20 Hz. Tests were conducted under load control at stress ratios of 0.1 (Ti-6-4) and 0.05 (TiAl). Tests were performed using the step-stress test method in which the sample was cycled for 10^6 cycles at each stress step. If failure had not occurred during this time period, the maximum stress level was increased by 28 MPa (4 ksi), and another block of 10^6 cycles was

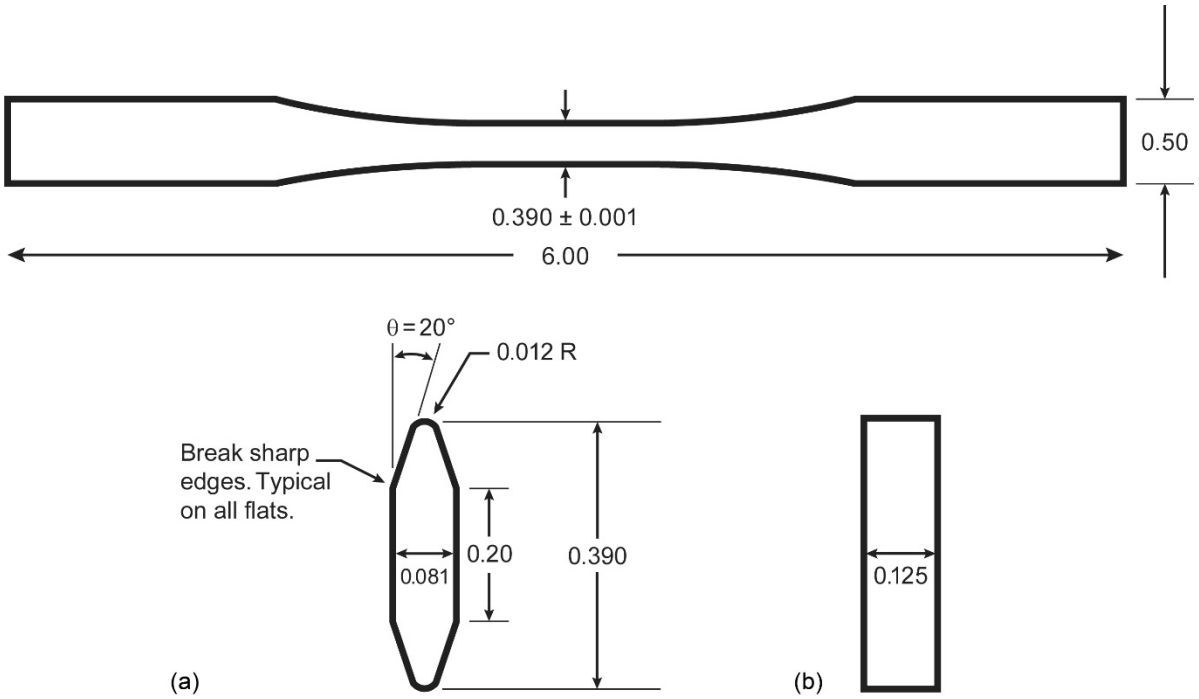

Figure 1.—Fatigue sample designs (dimensions in inches). (a) Elliptical gage cross section for TiAl, which includes leading edge. (b) Rectangular cross section for Ti-6Al-4V.

implemented. One exception to this occurred in the first fatigue test conducted on Ti-6-4 where a step increment of 14 MPa (2 ksi) was used. This process was continued until the sample failed. The fatigue life was given as the final cycle number at the maximum stress on the final loading block. The fatigue endurance limit is the maximum stress from the penultimate block, which ran out at 10^6 cycles. The step test process was investigated in another study (Ref. 6) and shown to give good values for the endurance limits.

Results

A description of the coating morphology is presented. Thereafter, the fatigue behavior of both Ti-6-4 and TiAl is shown. Fractography and metallography allowed observations of coating cracks and spallation due to the mechanical loads.

Morphology

Figure 2 shows a scanning electron microscopy (SEM) image of the TiCrAlTaSiN coating that was deposited on a titanium-alloy substrate. It was subsequently exposed in air for 100 h at 800 °C to oxidize the surface. The energy dispersive spectroscopy (EDS) analysis showed the approximate atomic composition ratios (Ti:Al:Cr:Ta:Si, excluding N) on this top layer as approximately 1.0:1.0:0.86:0.27:1.25.

Figure 3 shows backscattered SEM cross section images of the TiAlCrTaSiN/TiAlCrSi two-layer coating system (i.e., the top multicomponent nitride layer and inner TiAlCrSi barrier layer) on Ti-6-4 and TiAl alloy substrates. The coatings generally showed excellent adhesion after PVD processing. It can be seen that at the surface top coat has a columnar structure morphology, typical of the PVD process. It can

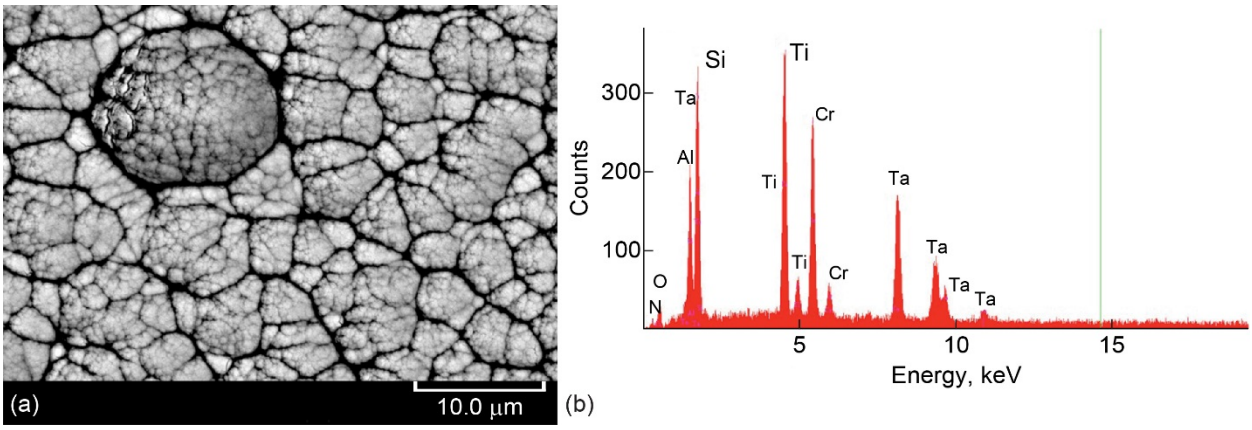

Figure 2.—TiCrAlTaSiN coating (top coat), preoxidized for 100 h at 800 °C. (a) Scanning electron microscopy (SEM) image of surface morphology. (b) Energy dispersive spectroscopy (EDS) spectrum.

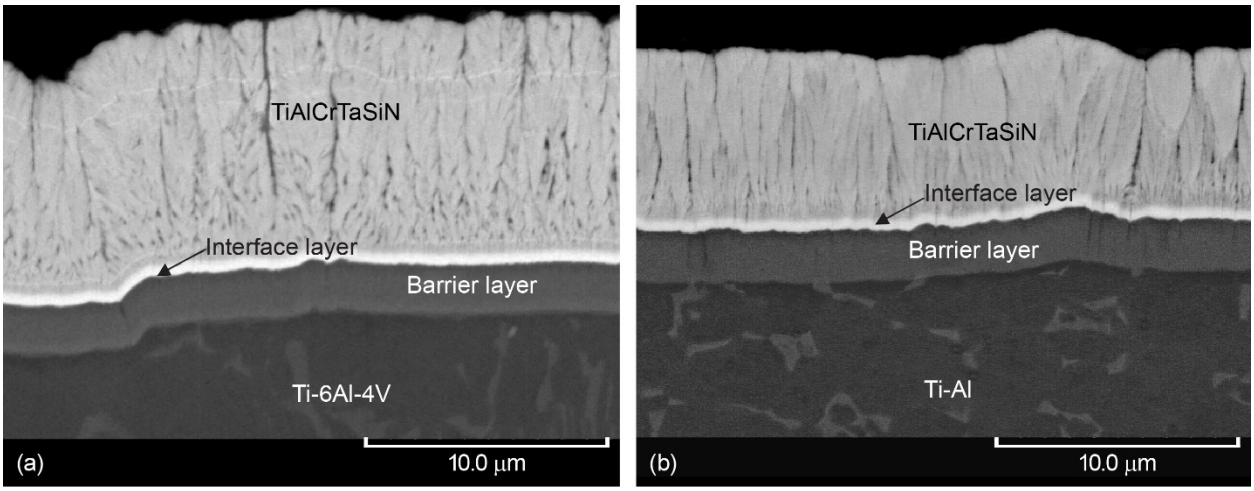

Figure 3.—Scanning electron microscopy (SEM) backscattered images of cross section of TiAlCrTaSiN/TiAlCrSi coating system on Ti-based substrates. (a) Ti-6-4 substrate. (b) TiAl substrate.

also be seen that a dense, bright interface layer formed between the top coat nitride layer and the bond coat barrier layer. An EDS analysis showed this interface layer to be rich in tantalum, and may be a consequence of depositing excessive Ta as the composition was transitioned from the non-Ta containing bond coat to the Ta-containing top nitride layer.

Ti-6Al-4V

Seven samples were tested in the uncoated condition to establish a baseline fatigue strength. The fatigue lives and endurance limits are given in Table I. The uncoated Ti-6-4 yielded an average maximum endurance limit strength of 504 MPa (73 ksi) with a 28-MPa standard deviation. These data agree with some cylindrical Ti-6-4 samples run under similar conditions for a study on damage modeling at NASA (Ref. 7). By coating the samples, the average maximum endurance limit strength dropped to 359 MPa (52 ksi) (with a standard deviation of 14 MPa)—a reduction of nearly 30 percent. A typical failure of the uncoated specimens is shown in Figure 4, where the fatigue crack started at the edge of the sample

(arrow) from a single, small initiation site. There were very few, if any, secondary cracks observed along the gage length. In contrast, the eight coated samples exhibited many crack initiation sites along the edge (Figure 5) and on the face, emanating from the coating. Examination of the gage section revealed multiple surface coating cracks (arrows) running perpendicular to the applied stress axis. The elastic mismatch between the relatively hard coating system and the soft (particularly at 427 °C) Ti-6-4 substrate results in a large strain mismatch, resulting in more coating-induced surface crack initiations and a subsequent reduction in fatigue life.

TABLE I.—FATIGUE RESULTS FOR UNCOATED AND COATED Ti-6Al-4V ALLOY SAMPLES

(a) Uncoated

Sample	Endurance limit, MPa	Fatigue life	
		Max. stress, MPa	Life, cycles
T13	455	469	153,167
T14	483	510	95,013
T15	483	510	51,318
T16	510	538	65,597
T17	538	565	65,597
T18	538	565	47,362
T19	510	538	53,967

(b) Coated

Sample	Endurance limit, MPa	Fatigue life	
		Max. stress, MPa	Life, cycles
C1	(a)	400	88,064
C2	(a)	400	50,839
C3	372	400	62,123
C4	345	372	104,892
C5	345	372	82,792
C6	345	372	96,321
C7	372	400	55,766
C8	345	372	102,305

[a]Failed in first load block.

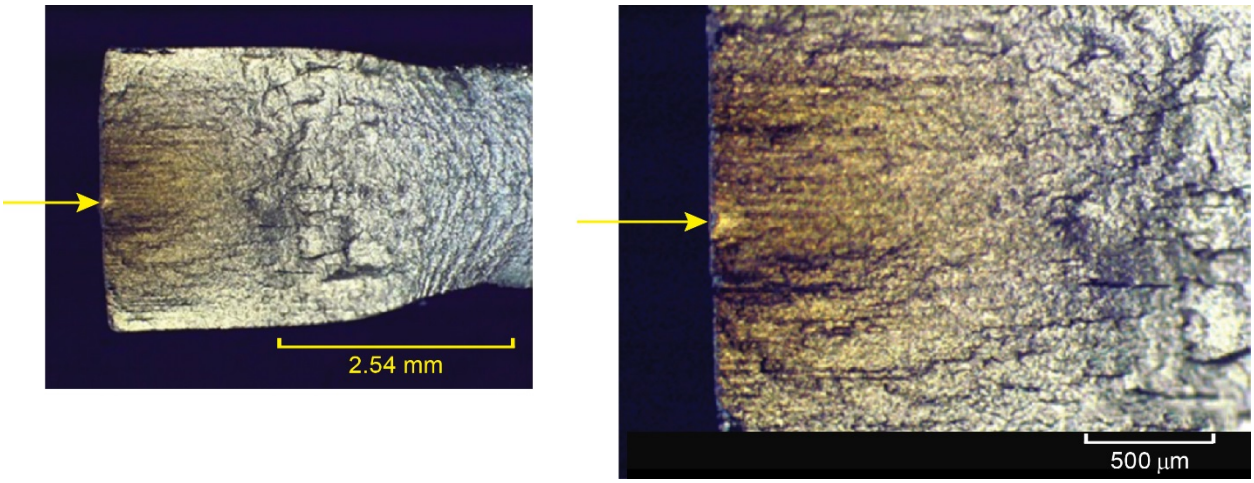

Figure 4.—Optical image of fracture surface of uncoated Ti-6Al-4V sample. Load axis is out of plane. Arrow shows singular crack initiation site at sample's edge. (a) Low magnification. (b) Higher magnification.

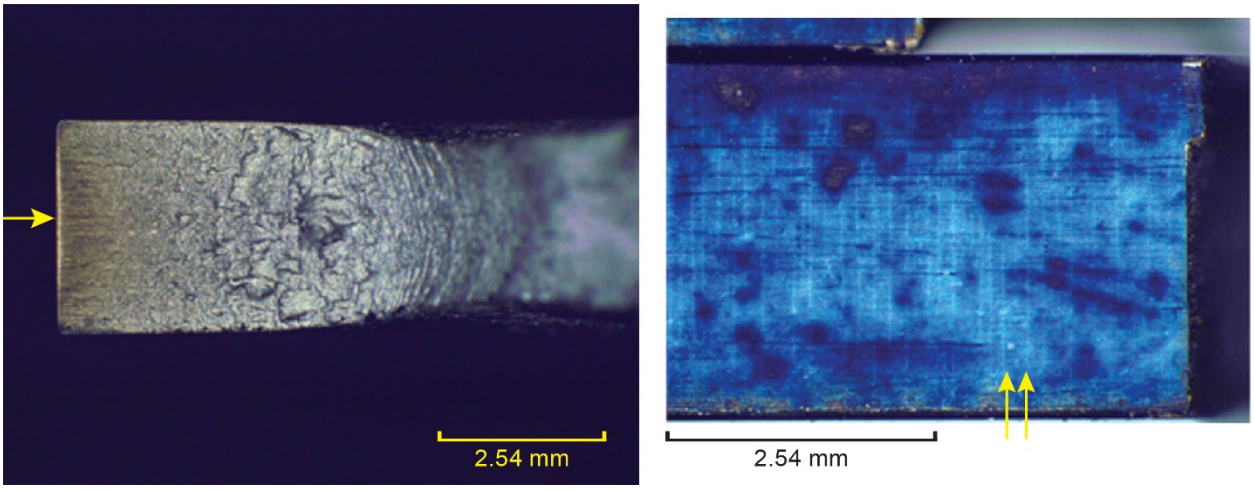

Figure 5.—Optical image of fracture surface of Ti-6Al-4V sample with TiAlCrTaSiN/TiAlCrSi coating. (a) Arrow depicts crack emanating from coating on edge. Load axis is out of plane. (b) Arrows depict transverse coating cracks on sample surface; load axis is horizontal.

GMPX TiAl

Seven coated TiAl samples were tested to failure and their results are shown in Table II. Out of these seven samples only six sustained a penultimate block, which ran out at 10^6 cycles. The average maximum endurance limit strength for these six samples was 600 MPa (87 ksi) with a standard deviation of 90 MPa (13 ksi). The standard deviation is 6.4 times that of the coated Ti-6-4 and is an indication of the brittle, defect-sensitive nature of TiAl. Crack initiation in these samples started at the leading or beveled edge of the sample (Figure 6). These locations are similar to those observed in an earlier study on the uncoated material (Ref. 2). The uncoated samples had an endurance limit of 573 MPa (83 ksi) with a standard deviation of 124 MPa (18 ksi). It should be noted that there were only three samples tested in the uncoated state, and at least two of them (11-6 and 11-12) had diminished endurance limits due to tiny flaws in the TiAl. It is estimated that the defect-free endurance limit should be at least as high as 711 MPa (103 ksi), based on results from the third sample (11-5) and extrapolation of the curves in Reference 2

showing limit stress versus defect size. Given this, the reduction in the endurance limit for the coated TiAl should be around 20 percent.

It was observed on failed samples that the coating had spalled and the gage section contained numerous, evenly spaced cracks (Figure 7). The outer coating had limited adhering capability under load and spalled readily, possibly due to its high stiffness and low toughness. To ensure that this was not just a result of a thermal expansion mismatch between the coating and the substrate, a sample was heated to the fatigue test temperature of 650 °C, under zero load for 1 h, cooled to room temperature, and then examined under an optical microscope. No spalling or cracking of the coating was observed. In an attempt to mitigate the problem with the outer coating, another sample was heat treated in a furnace at 650 °C for 96 h in an attempt to reduce any residual stresses. After the thermal treatment, the coating was again examined and found to be in excellent condition. This sample, 11-9, was then fatigue tested. The thermal treatment had no effect on the coating adherence as cracking and spallation were still observed (Figure 7). In fact, it should be noted that this sample had the lowest endurance limit of the group, suggesting that the existing coating still is not sufficiently optimized to provide suitable protection for the TiAl. The fatigue results are summarized in Figure 8 for both alloys. The three points with the error bars represent the range of fatigue endurance limits (i.e., runouts at 10^6 cycles) for the respective materials. At stresses near the endurance limit, it is not unusual for some samples to fail while others reach the endurance limit, as a result of the inherent scatter in the material. It should be pointed out that the coated TiAl still exhibit better fatigue strengths compared to those of Ti-6-4 in spite of the degradation that the coating provoked and its higher test temperature. Thus, there is still promise for this coating system.

TABLE II.—FATIGUE RESULTS FOR UNCOATED AND COATED GAMMAMET PX TiAl ALLOY SAMPLES

(a) Uncoated

Sample	Endurance limit, MPa	Fatigue life	
		Max. stress, MPa	Life, cycles
11-6	483	510[a]	9,120
11-5	710	738	868,160
11-12	510	538[a]	16,080

(b) Coated

Sample	Endurance limit, MPa	Fatigue life	
		Max. stress, MPa	Life, cycles
11-9	441	469	557,912
11-7	662	690	446,260
11-11	607	634	1,649
11-13	579	607	2,556
11-14	690	717	1,746
11-15	634	662	1,543
11-10	(b)	496	2,533

[a]Contained small flaws in TiAl.
[b]Failed in first load block.

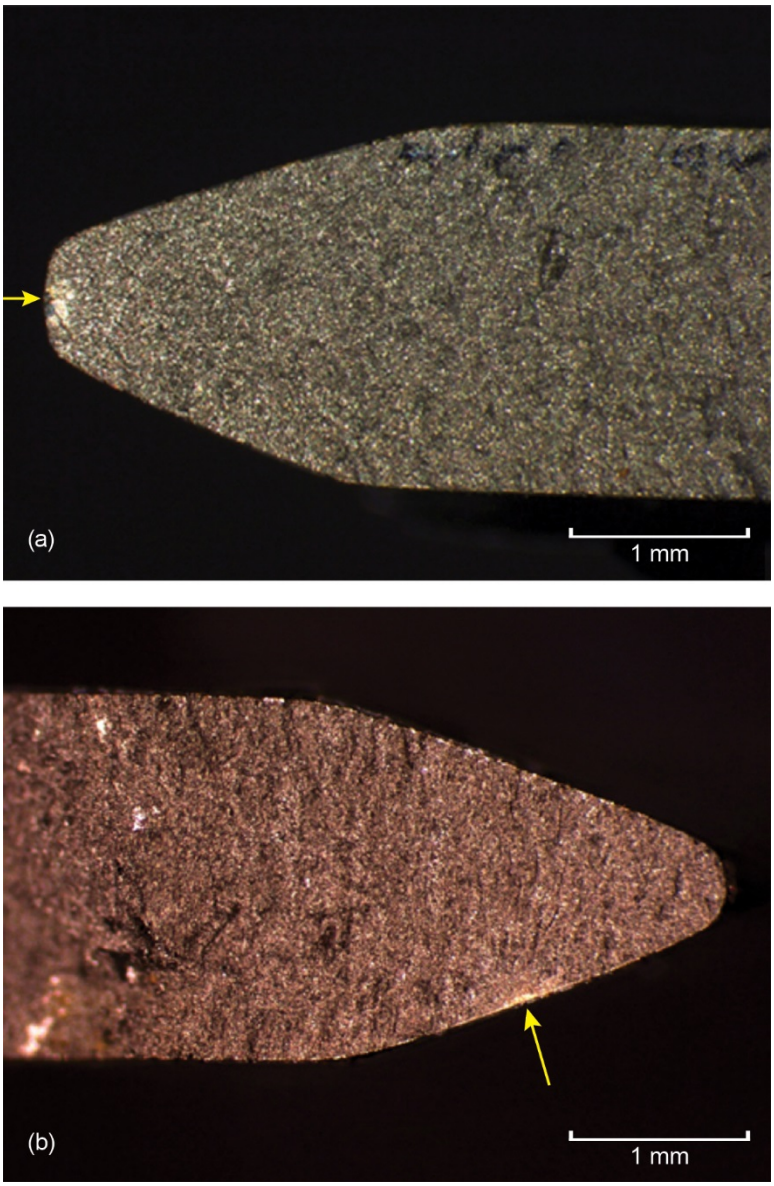

Figure 6.—Optical image of fracture surface of TiAl specimens with TiAlCrTaSiN/TiAlCrSi coating. Arrows show initiation sites. Load axis is out of plane. (a) Sample 11-13. (b) Sample 11-14.

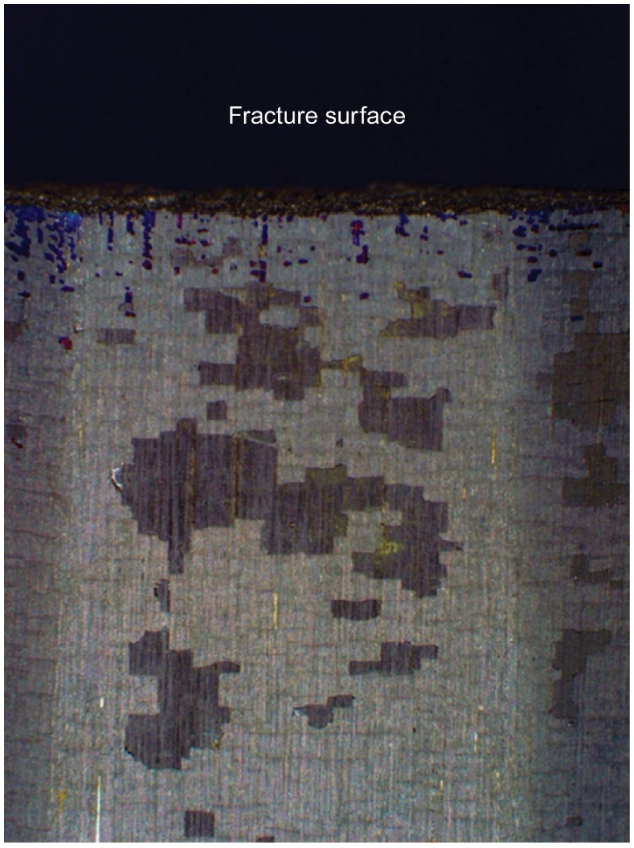

Figure 7.—Top coat of gage section of TiAl sample with TiAlCrTaSiN/TiAlCrSi coating 11-9 cycled to maximum stress of 469 MPa (68 ksi). Load axis is vertical.

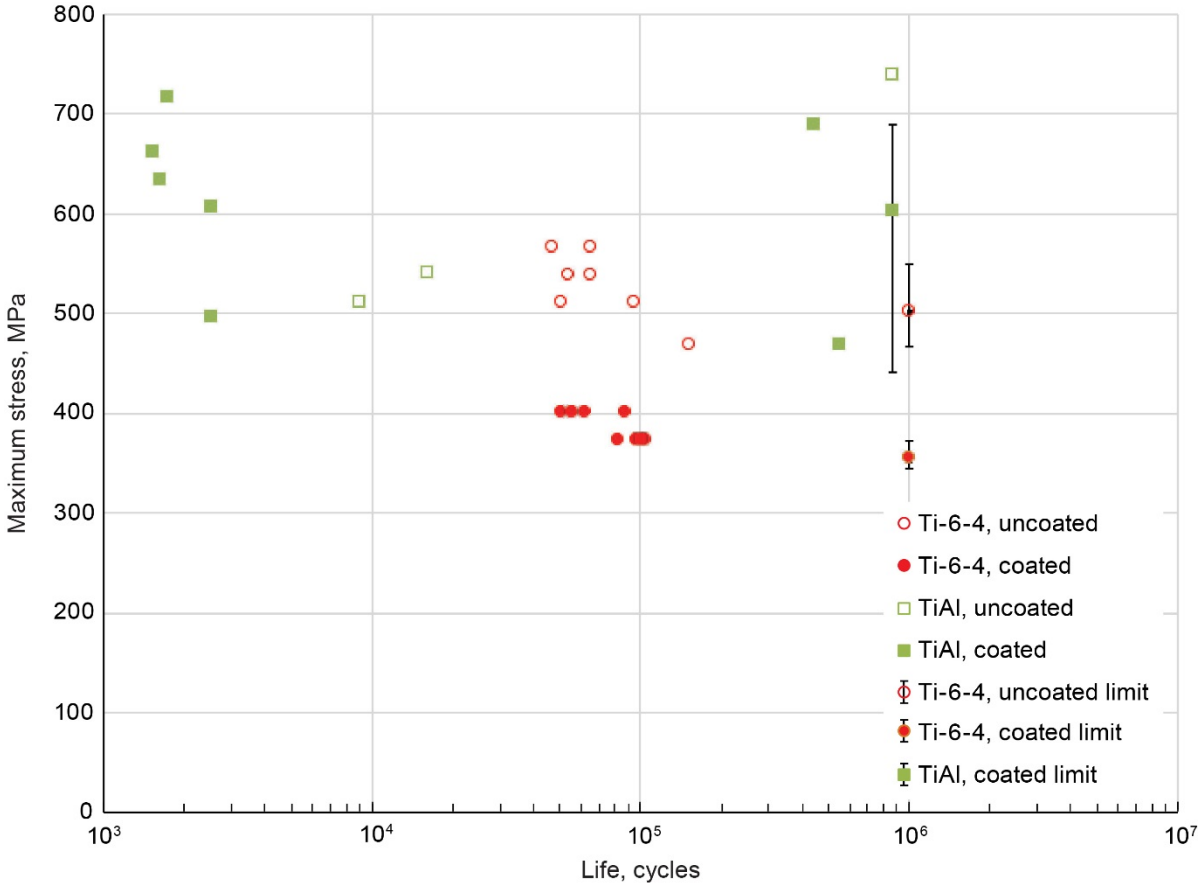

Figure 8.—Fatigue behavior of Ti4-6Al-4V and GammaMet PX TiAl, uncoated and with TiAlCrTaSiN/TiAlCrSi coating. Values of fatigue limits and associated variations are also shown with vertical bars.

An attempt was made to determine if there was a limit load in the coated TiAl below which no coating cracks formed. Therefore, samples were tested at various starting load levels. Even at a cyclic stress of only 221 MPa (32 ksi)—the lowest maximum stress attempted—the coating exhibited cracks after experiencing 10^6 cycles. Figure 9 is an optical micrograph of the gage showing such cracks in this sample. Although there are significantly fewer cracks in this sample than those observed at a higher stress (Figure 7), the coating still cracks. Figure 10 is a photograph of the leading edge of the low-stress sample, which displays more transverse cracks. This result emphasizes the need for more ductility in this particular coating system.

Figure 11 is a secondary electron SEM image showing cracking in the coating and in the substrate (arrows) for the same low-stress sample. There are cracks also running in the longitudinal direction in the top coating. In Figure 9, Figure 10, and Figure 11 the loading direction is along the horizontal direction of the page, which is also the longitudinal direction for the specimens. The vertical direction of the page is perpendicular to the loading direction and represents the transverse (or width) direction of the test specimen.

Figure 12 shows SEM backscattered cross-sectional images of TiAl test sample 11-7, depicting the surface coating cracking and the delamination in the TiCrAlTaSiN top coat close to the Ta interface layer, after the highly loaded conditions (endurance limit 662 MPa or 96 ksi, failure at 690 MPa or 100 ksi, and 446,260 fatigue cycles). Some delamination of the metal-rich TiAlCrSi also was observed at failure. An enlarged magnification shown in Figure 12(b), suggests that the substrate was still protected from oxidation, since the microstructure of the TiAl substrate remained mostly unchanged and hence, prevented initiation of any of cracks in the substrate. The EDS analysis shown in Figure 12(c) also showed that the various coating layers had chemical compositions as designed, especially those with high aluminum contents.

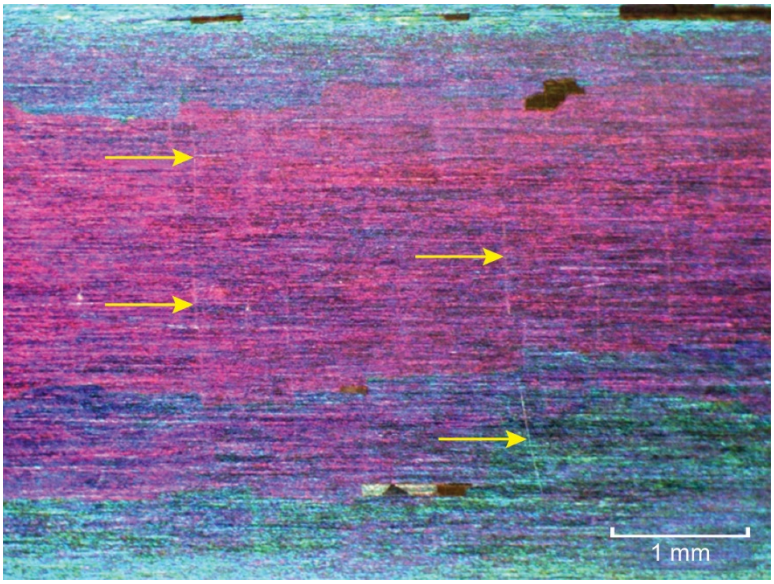

Figure 9.—Optical micrograph of TiAl sample with TiAlCrTaSiN/TiAlCrSi coating, showing transverse cracking (arrows) after experiencing 10^6 load cycles with maximum stress of 221 MPa (32 ksi). Load axis is horizontal.

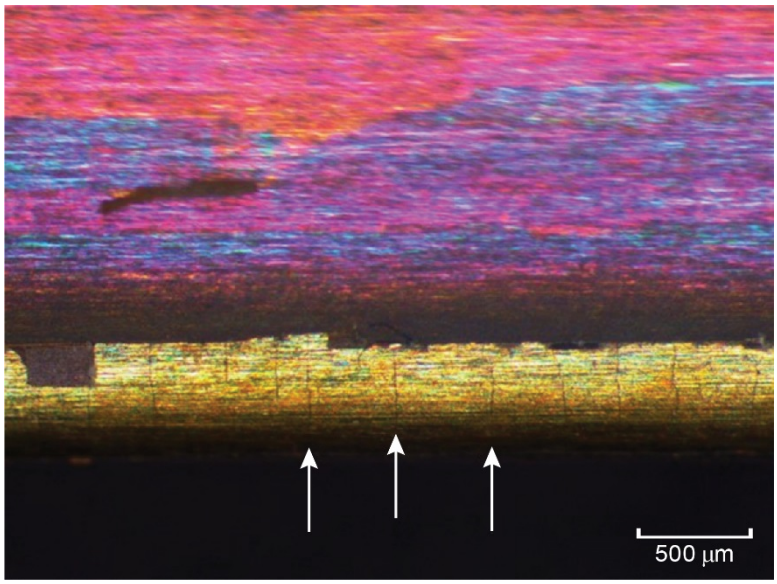

Figure 10.—Optical micrograph of leading edge of coated TiAl sample with TiAlCrTaSiN/TiAlCrSi coating, showing surface layer coating cracks for sample cycled at 221 MPa (32 ksi). Load axis is horizontal.

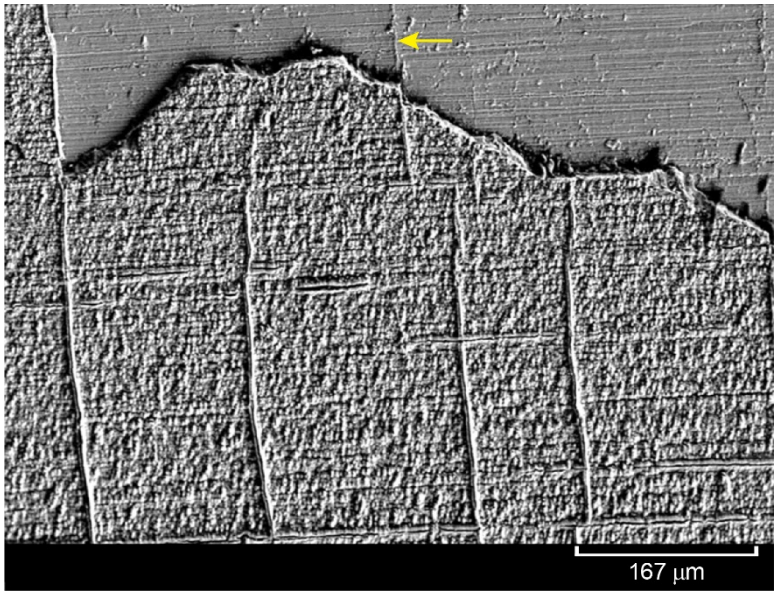

Figure 11.—Secondary electron scanning electron microscopy (SEM) image of TiAl sample with TiAlCrTaSiN/TiAlCrSi coating, showing cracks in substrate (arrow) and coating (in both transverse and longitudinal directions) after fatigue testing at maximum stress of 221 MPa. Load axis is horizontal.

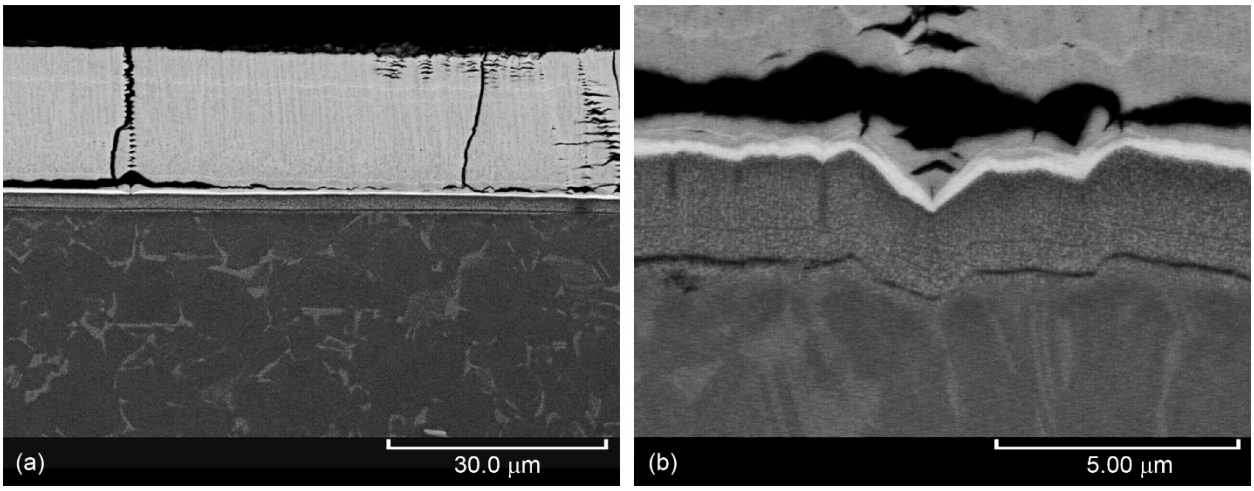

Figure 12.—Scanning electron microscopy (SEM) backscattered cross section images of TiAl sample with TiAlCrTaSiN/TiAlCrSi coating 11-7 cycled to maximum stress of 690 MPa (100 ksi). (a) The coating, showing top coat cracking and delamination along interface coating layer. (b) Enlarged interface region between coatings. (c) Energy dispersive spectroscopy (EDS) analysis of top coat (EDS A), Ta-rich interface layer (EDS B and C), and metal-rich barrier coating (EDS D).

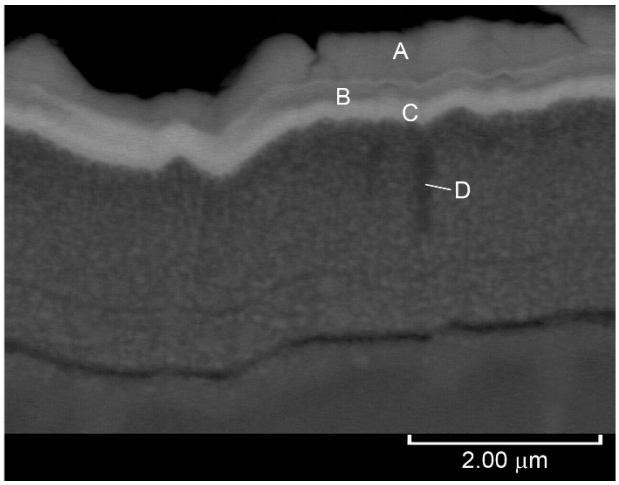

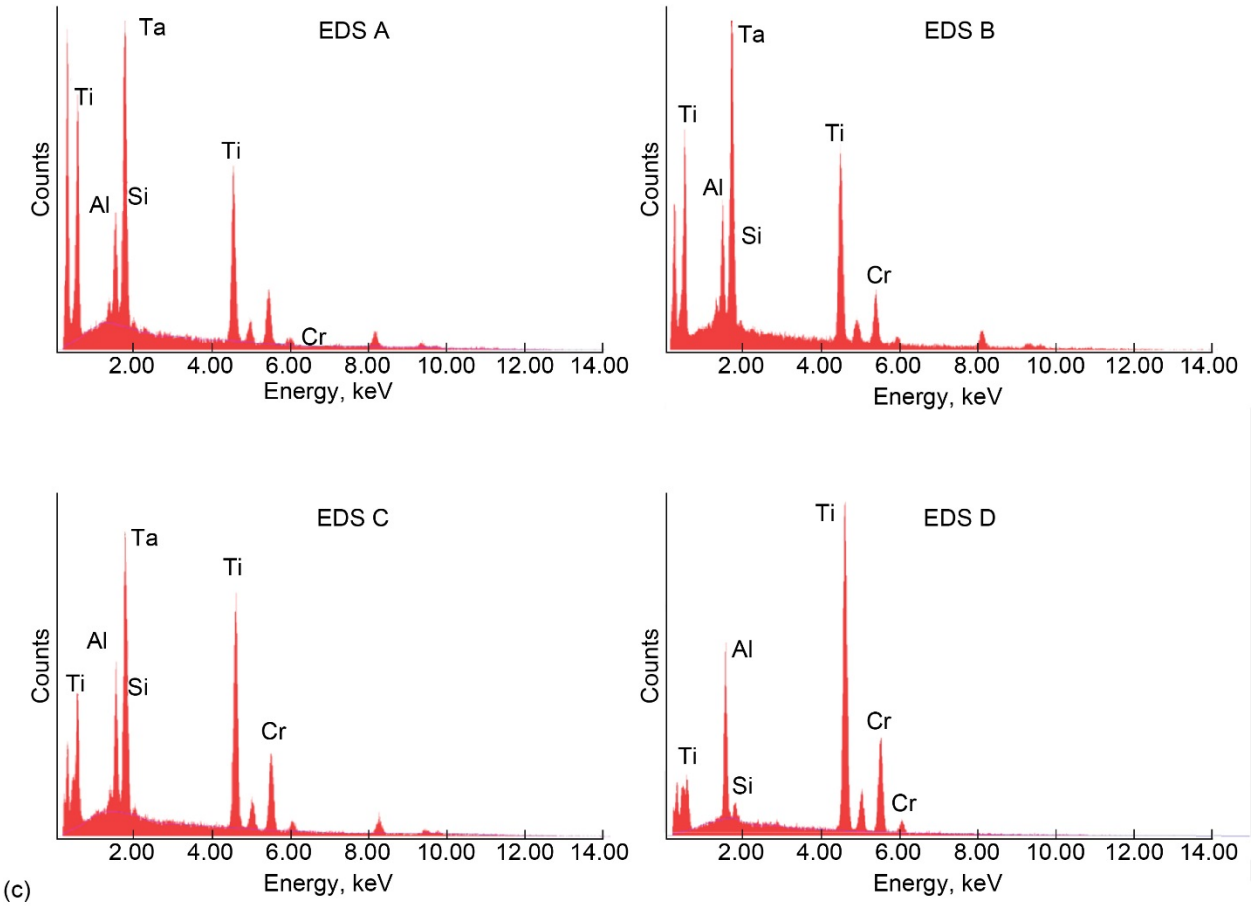

(c)

Figure 12.—Concluded.

Because the coating consists of a two-layer ceramic-metal system, sometimes processing defects can induce weak coating interfaces that can cause cracking and spallation within the layers. In general, the weakest interfaces are found at the transition interfaces between the wear-impact ceramic-based top coating and the oxidation-resistant TiAlCrSi bottom coating. However, Figure 13 shows a delamination at midcoating thickness in the top layer, which could be due to a processing defective interface within the ceramic coating. Transverse cracks can also be observed in this coating, as well as a substantial amount of oxidation. Note however, that the inner, metal-rich coating seems still relatively intact, even though there is some indication of slight oxidation at the metal interface. Nevertheless, this specimen (11-9) still completed 557,912 fatigue cycles after the 100-h pretest oxidation exposure. Figure 14 and Figure 15 show backscattered SEM images of the gage surface from some earlier batch-coated, TiAl samples after fatigue testing. The separation or delamination within the topcoat layer occurred during the fatigue loading because of the weak interface (Figure 14). EDS shows the coating composition at various locations through the thickness. Of particular note are the areas of carbon at various places (see Figure 14, EDS C)—carbon was observed within the coatings and also at coating interfaces. The inner TiAlCrSi coating (EDS Area B) seemed still intact after 100 h oxidation and subsequent fatigue testing. The carbon contamination may be from coating processing, which would result in the observed delamination of the top coat. In Figure 15, one can see that the composition of both the metallic bond coat (EDS A) and the ceramic top coat (EDS D and E) exhibit very low aluminum contents and are not representative of expected coating compositions. Thus, there appears to be various processing-related problems that need to be resolved. Chemical analysis of the top coat also shows large amounts of oxygen, presumably SiCr(TiTa) oxide.

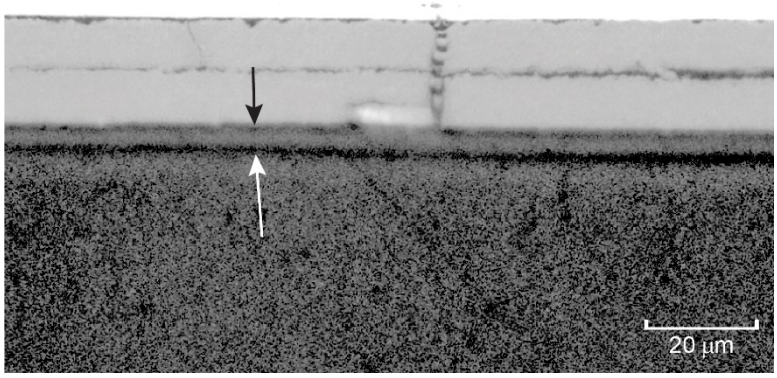

Figure 13.—Optical micrograph of oxidized top coat (arrows) of TiAl sample with TiAlCrTaSiN/TiAlCrSi coating, showing transverse cracks and delamination in 11-9 cycled to maximum stress of 469 MPa after pretest oxidation (100 h at 800 °C). Loading axis is horizontal.

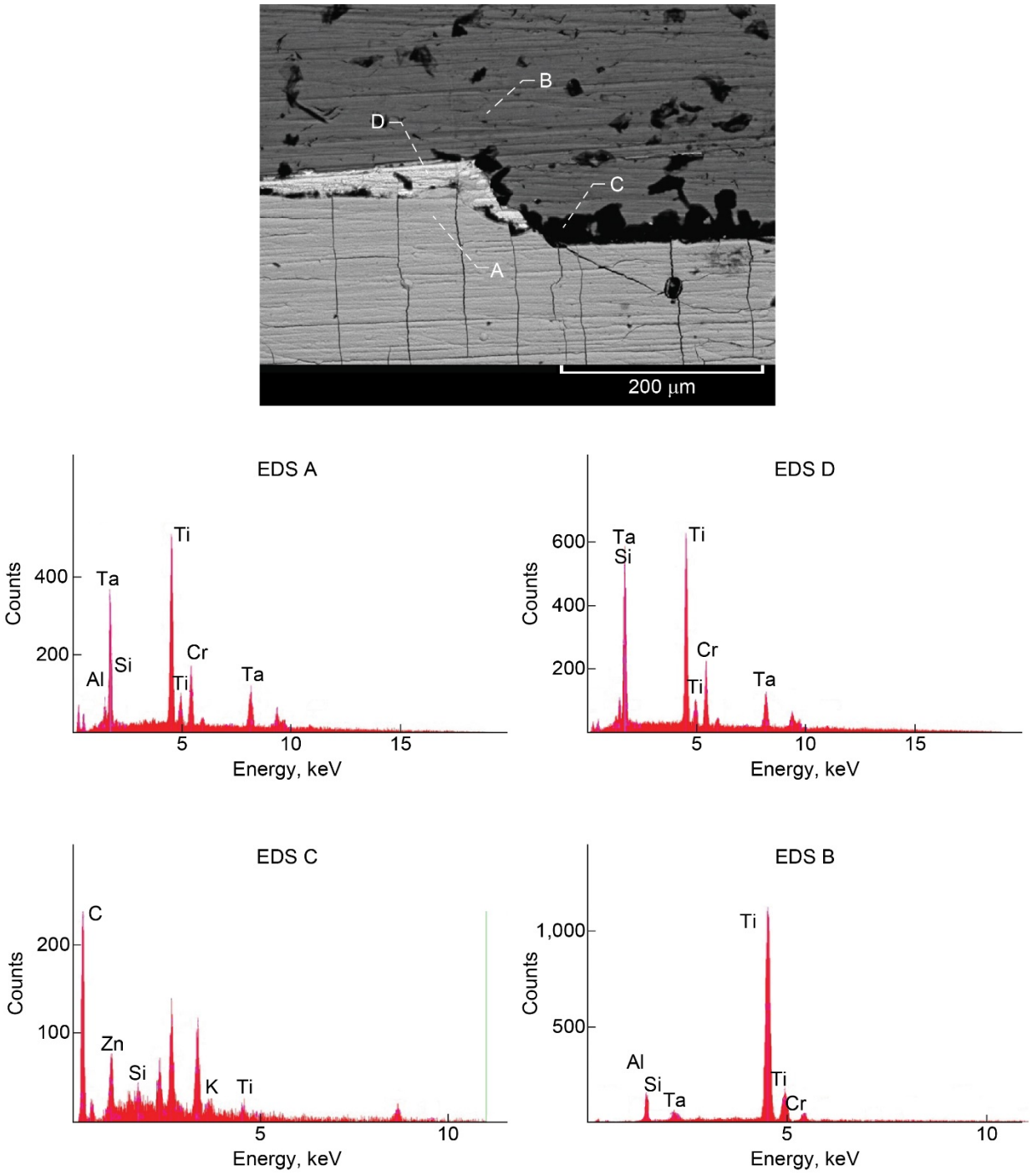

Figure 14.—Scanning electron microscopy (SEM) image and energy dispersive spectroscopy (EDS) spectra of TiAl sample with TiAlCrTaSiN/TiAlCrSi coating, showing surface coating cracking. Photomicrograph of coating, with top coating cracking and delamination along interface coating layer. EDS A shows composition of top coat. EDS D shows delamination at top coat. EDS C shows carbon contamination at interface between top and bond coat. EDS B shows composition near bond coat.

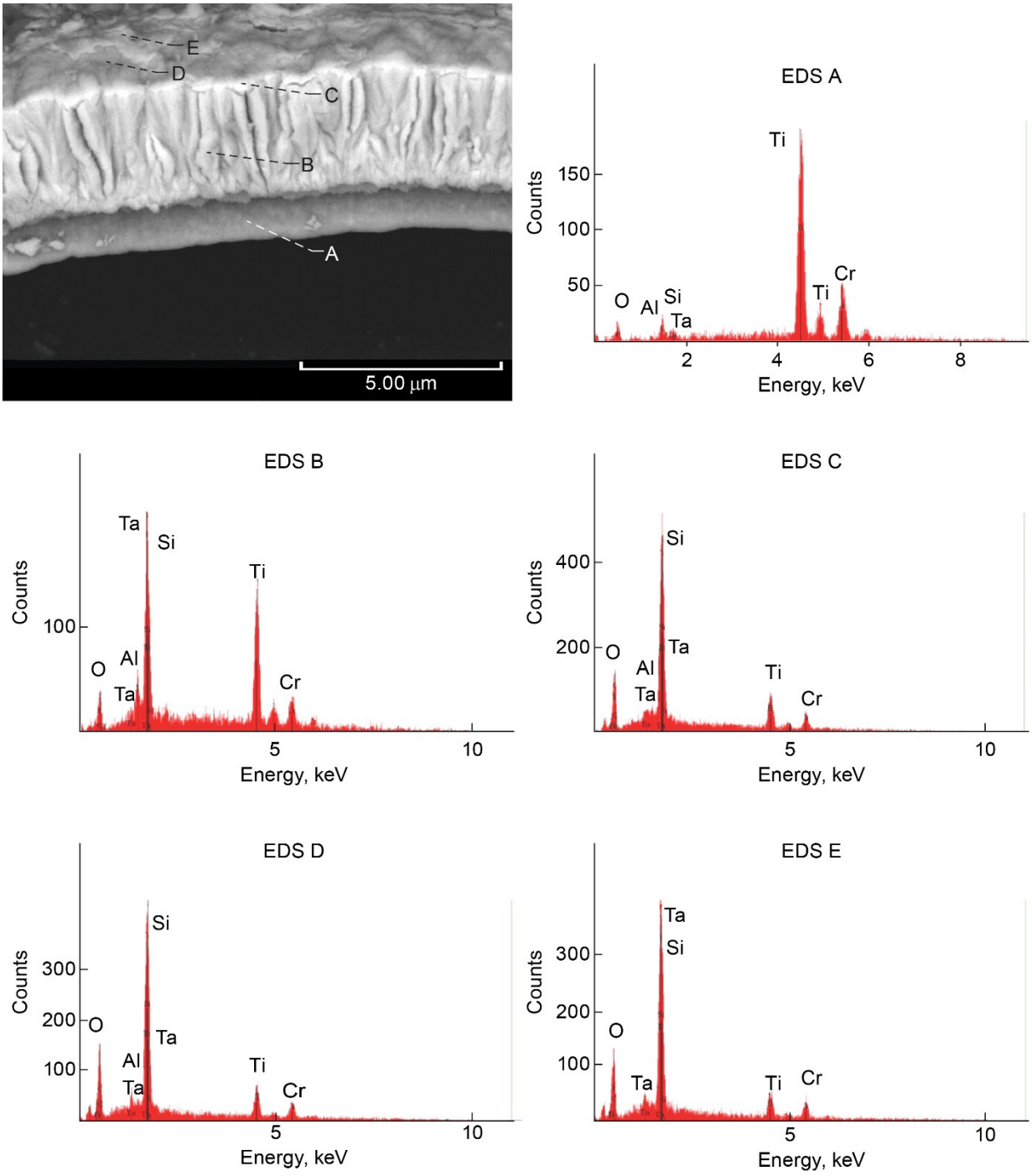

Figure 15.—Scanning electron microscopy (SEM) fracture surface backscattered image and energy dispersive spectroscopy (EDS) analysis of fatigue-tested coated TiAl with TiAlCrTaSiN/TiAlCrSi coating, showing thin oxidation barrier layer (EDS A), Ta-rich interface layer (EDS B and C), and top coat (EDS D and E).

Discussion

The coating was shown to decrease the endurance limit of both Ti-6-4, and possibly TiAl (defect free) by 30 and 20 percent, respectively. Although for TiAl, because of a small number of uncoated sample data, and intrinsically large scatter of the brittle intermetallic alloy, the finding may not be very conclusive. For the Ti-6-4 material the test temperature (427 °C) was high and out of the range of most applications for this material. The temperature was chosen to be consistent with another NASA program (Ref. 7) on this alloy. At 427 °C the alloy is very ductile. Under load-controlled fatigue testing with a load ratio of 0.1, the samples undergo strain ratcheting, in which the specimen continually elongates because of time-dependent processes under the tensile mean stress. This was observed by the continual increase in the displacement measurements as given by the loading actuator displacement. The high ductility is also evidenced by the reduction of area observed at the fracture surfaces. The high deformation of the base alloy was originally suspected to be the reason for poor coating performance and loss of fatigue strength, since it strains more than the brittle coating. However, the tests on TiAl may suggest additional reasons.

Contrary to Ti-6-4, TiAl is an intermetallic with limited ductility, even at the high test temperature of 650 °C. The strain to failure of this material was shown to be 1.9 percent (Ref. 2) at 650 °C. Hence, a high-stiffness coating like the TiAlCrTaSiN/TiAlCrSi system used in this study should have better strain compatibility with TiAl compared to Ti-6-4 and is expected to protect the substrate better. However, use of the coating on the TiAl still reduced the fatigue strength albeit to a lesser extent than for Ti-6-4. The fatigue strength of gamma TiAl alloys such as GMPX are highly influenced by defects (Refs. 1, 8, and 9), and their failure can be regularly predicted above a certain defect size by linear elastic fracture mechanics. At very small defect sizes, the fatigue strength can still be reduced as was indicated in this study (see, for example, samples 11-6 and 11-12 in Table II). As shown in Figure 6 and Figure 7, cracks in the coating can act as defects and eventually propagate into the TiAl substrate, particularly if the TiAlCrSi bond coat does not have sufficient toughness to blunt the cracks and prevent continued propagation of the top coating cracks, thus reducing the overall fatigue strength. Insufficient oxidation protection can also result in early crack initiation within the substrates, leading as well to a reduction in fatigue strength. Interrupted tests have shown that the top ceramic coating cracks can form at very low fatigue stresses. This study revealed that the cracks existed after 10^6 cycles at a maximum stress of only 221 MPa (32 ksi). If a cracking threshold stress exists for the coating, it is still below this limit stress and was not pursued further. A maximum stress of 221 MPa (32 ksi) is already 31 percent of the expected fatigue limit strength of the uncoated (defect-free) material.

To see if cracking was strictly due to a CTE mismatch, a sample was held for 1 h at a temperature of 650 °C with no imposed load. It was then cooled and examined under an optical microscope. No cracks or other coating distress were observed. Therefore, we believe that the coating is failing due to its low ductility rather than a CTE mismatch. This is especially evident with the ductile Ti-6-4 substrates. The outer ceramic-based wear coating was also found to be easily prone to spallation. Attempts to improve its adherence through self-diffusion by annealing the sample at 650 °C for 96 h were unsuccessful. The erosion- and wear-resistant coating still spalled under subsequent cyclic loading. It was also observed that annealing under these conditions yielded the lowest fatigue strength of all of the coated TiAl samples, perhaps suggesting that the coating still may not have enough long-term oxidation protection. Overall, the effect of the coating system on the fatigue behavior of TiAl is complex; the inner oxidation barrier bond coat may be all that is needed for protecting the TiAl alloys in high-temperature oxidizing fatigue environments, if erosion is not an issue. The coating processing and compositional control also need to be further investigated as they appear to lead to occasional coating contamination as well as inhomogeneous and out-of-specification chemistries.

Summary and Future Work

This work suggests that coating compositions and especially processing improvements would be needed for Ti alloy coatings before they could be used in service under highly loaded fatigue and oxidation conditions. Although the current TiCrAlSi oxidation coating appears to work well with these two titanium alloys, the top erosion-resistant coating needs additional improvement. Its adherence and toughness are currently too poor to accommodate the highly loaded cycles typical of titanium turbine engine components. This is particularly true for TiAl, which is defect sensitive whereby small coating cracks can easily reduce its life. More advanced coating designs and systems are needed in order to provide sufficient protections from wear or erosion in the application of highly loaded components and in oxidation-erosion-impact conditions. Studies on large thermal cycles with and without concurrently applied loads will also have to be investigated.

References

1. Draper, S.L., et al.: Durability Assessment of Gamma TiAl—Final Report. NASA/TM—2004-212303, 2004. http://ntrs.nasa.gov
2. Draper, S.L., et al.: Microstructure and Mechanical Properties of Extruded Gamma Met PX. Presented at the Gamma Titanium Aluminides 2003, The Minerals, Metals and Materials Society, Warrendale, PA, 2003, pp. 207–212.
3. Musil, J.: Hard Nanocomposite Coatings: Thermal Stability, Oxidation Resistance and Toughness. Surf. Coat. Tech., vol. 207, 2012, pp. 50–65.
4. Wei, R.: Plasma Enhanced Magnetron Sputtering Deposition of Superhard, Nanocomposite Coatings. Plasma Surface Engineering Research and Its Practical Applications, R. Wei, ed., Research Signpost, 2008, pp. 87–115.
5. Zhu, Dongming; and Hurst, Janet B.: Advanced High Temperature and Fatigue Resistant Environmental Barrier Coating Bond Coat Systems for SiC/SiC Ceramic Matrix Composites. Patent Application 2013/0344319 A1, Dec. 26, 2013.
6. Lerch, B.A.; Draper, S.L.; and Pereira, J.M.: Conducting High-Cycle Fatigue Strength Step Tests on Gamma TiAl. Metall. Mater. Trans. A, vol. 33, no. 12, 2002, pp. 3871–3874.
7. Lerch, B.A.; and Arnold, S.M.: An Exploration of Failure and Potential Damage Markers in Ti-6Al-4V. NASA/TM—2018-219902, 2018. http://ntrs.nasa.gov
8. Harding, Trevor S.; and Jones, J. Wayne: The Effect of Impact Damage on the Room-Temperature Fatigue Behavior of γ-TiAl. Metall. Mater. Trans. A, vol. 31, no. 7, 2000, pp. 1741–1752.
9. Chan, K.S.; and Shih, D.S.: Fundamental Aspects of Fatigue and Fracture in a TiAl Sheet Alloy. Metall. Mater. Trans. A, vol. 29, 1998, pp. 73–87.